Unclassified
SECURITY CLASSIFICATION OF THIS PAGE

(2)

DOCUMENTATION PAGE

Form Approved
OMB No. 0704-0188

AD-A222 340

DTIC
ELECTE
MAY 30 1990
B CD

1b. RESTRICTIVE MARKINGS

3. DISTRIBUTION/AVAILABILITY OF REPORT
Approved for public release: Distribution is unlimited

2b. DECLASSIFICATION/DOWNGRADING SCHEDULE

4. PERFORMING ORGANIZATION REPORT NUMBER(S)

5. MONITORING ORGANIZATION REPORT NUMBER(S)
AFOSR-TR- 90-0528

6a. NAME OF PERFORMING ORGANIZATION	6b. OFFICE SYMBOL (If applicable)	7a. NAME OF MONITORING ORGANIZATION
Wayne State University		AFOSR/NP

6c. ADDRESS (City, State, and ZIP Code)	7b. ADDRESS (City, State, and ZIP Code)
565 West Kirby Detroit, MI 48202	Building 410 Bolling AFB, DC 20332-6448

8a. NAME OF FUNDING/SPONSORING ORGANIZATION	8b. OFFICE SYMBOL (If applicable)	9. PROCUREMENT INSTRUMENT IDENTIFICATION NUMBER
AFOSR	NP	Contract: F49620-86-C-0079DEF

8c. ADDRESS (City, State, and ZIP Code)	10. SOURCE OF FUNDING NUMBERS			
	PROGRAM ELEMENT NO.	PROJECT NO.	TASK NO.	WORK UNIT ACCESSION NO.
Building 410 Bolling AFB, DC 20332-6448	6322IC	D812	F1	

11. TITLE (Include Security Classification)
Diagnostics for hydrogen atoms and molecules in H-Atom sources and beams using VUV laser light

12. PERSONAL AUTHOR(S)
Erhard Rothe

13a. TYPE OF REPORT	13b. TIME COVERED	14. DATE OF REPORT (Year, Month, Day)	15. PAGE COUNT
Final Technical	FROM 9/1/86 TO 12/31/89	1990 April 24	25

16. SUPPLEMENTARY NOTATION

17. COSATI CODES			18. SUBJECT TERMS (Continue on reverse if necessary and identify by block number)
FIELD	GROUP	SUB-GROUP	
	20.09		Neutral Beam, Ion Source Diagnostics, Laser Diagnostics

19. ABSTRACT (Continue on reverse if necessary and identify by block number)

An H^- source for high brightness H^- beams should have the lowest possible internal temperature T, because the beam-power density at a distance scales as 1/T. We determine local T inside a discharge with the use of a tunable ArF excimer laser that measures the populations of the lowest four rotational states of H_2 by means of (2+1) resonance enhanced multiphoton ionization (REMPI). The number of laser-created ions causes a proportional change of the discharge's electrical impedance. A calibration in room temperature H_2 (without a discharge) showed that the REMPI works well. Another objective is to monitor vibrationally excited molecules, $H_2(v)$, that are believed to be the primary origin of H^- within volume-type ion sources. We use the same apparatus and approach, but add a Raman shifter to change the laser wavelengths to those appropriate for (2+1) REMPI of $H_2(v)$.

20. DISTRIBUTION/AVAILABILITY OF ABSTRACT	21. ABSTRACT SECURITY CLASSIFICATION
☒ UNCLASSIFIED/UNLIMITED ☒ SAME AS RPT. ☐ DTIC USERS	Unclassified

22a. NAME OF RESPONSIBLE INDIVIDUAL	22b. TELEPHONE (Include Area Code)	22c. OFFICE SYMBOL
Lt. Col. J. Lupo	(202) 767-4 7	AFOSR/NP

DD Form 1473, JUN 86 — Previous editions are obsolete. — SECURITY CLASSIFICATION OF THIS PAGE

Unclassified

TABLE OF CONTENTS

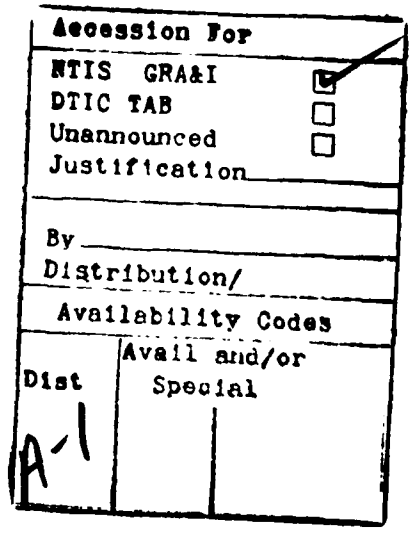

INTRODUCTION

This program has relevance to the NPB program of SDIO. In order to deliver as many H atoms (H^o) as possible to some distant target it is desired to have minimum divergence of the H^o-beam. Ultimately this reduces much of the problem to obtaining maximum intensity and minimum divergence (i.e., minimum value of a parameter known as the emittance) in the initial H^- ion source that provides the precursors for the neutral atoms. These parameters are combined in a figure of merit known as brightness.

The temperature T inside H^- ion sources should be as low as possible, because the transverse motions implied by a temperature serve to increase the emittance. The emittance, which is like the entropy of an isolated system, can increase (i.e., get worse) or stay the same, but it can not be reduced by such subsequent operations as ion focussing or acceleration. It can be shown that the energy density delivered to a distant target scales as 1/T if the emittance is limited by the ion source performance, which is now often true. A knowledge of the local T within a source would then help an ion-source designer optimize performance: e.g., through the elimination of "hot-spots" that cause unwanted increases of emittance.

Much of the ion source design may be characterized as "cut and try." It is not that the people working on these sources are not good at their jobs. Quite the opposite! But it is just the fact that the same group of good people have been adjusting similar knobs for up to 15 years that suggests that a more fundamental approach should help.

The present research is intended to help develop diagnostics. Obviously if the NPB program can reach its goals without further diagnostics then will not be needed. And there clearly are limited diagnostics in place, i.e., methods to measure current and emittance. However after 15 years of experimentation, and modelling, many of the most basic features of the Dudnikov source operation, or of the

volume source, (the program's major candidates) are basically still not understood. That means that any effort to improve performance of existing sources or to design improvements into new ones is something of a shot in the dark. We describe below two different sets of diagnostics. They use a similar method and are for 1) measurement of local temperatures and 2) measurements of vibrationally excited H_2. These are discussed in Sections 1 and 2 below.

1. TEMPERATURE MEASUREMENTS

PRINCIPLE

Our approach is to measure a rotational T in various locations within a discharge via (2+1) resonance enhanced multiphoton ionization [i.e., (2+1) REMPI] in H_2.[1,2] The (2+1) here means a two-photon excitation from a rotational level i in the ground (X) electronic and vibrational (v=0) states to levels of the E,F electronic state and an additional photon that ionizes from the E,F state. A given state yields a number of ions that is proportional to the density of i, n_i. Therefore in a neutral gas only a simple current measurement is needed. In a discharge these ions produce a proportional impedance change that can be easily measured: this is an optogalvanic effect.

For two different i, that have energies E_i and rotational quantum numbers j_i, we convert the corresponding n_i to T by means of the Boltzmann equation. This assumes local thermal equilibrium.

If the experimental ion signals S_i are proportional to the n_i, then

$S_1/S_2 = [(2j_1+1)(2T_1+1)]/(2j_2+1)(2T_2+1)]\exp-[(E_1-E_2)/kT]$, or

$T = [(E_2-E_1)/k] \ln\{[S_2(2j_1+1)(2T_1+1)]/[S_1(2j_2+1)(2T_2+1)]\}$,

where T_i is the nuclear spin degeneracy and is 1 and 3 for even and odd values of j_i, respectively.

This example used only two states. The use of more rotational states improves the accuracy and provides a consistency check.

Two-photon excitation occurs only where the light is focussed, and at the time of the laser pulse. The result is that temperature is measurable at desired locations within a discharge as well as at specific times (e.g., relative to the ion source pulse times). The measured rotational temperatures should be in equilibrium with the H^- temperature that is of direct interest. Even if there were deviations from this reasonable expectation, the relative n_i from position to position within the source will still be useful as a diagnostic.

We use four H_2 transitions, to the E-state, that lie within the 193nm ArF band. That band is only ≈0.7nm wide, but within that range are two-photon resonant transitions that originate from j_i = 0, 1, 2, and 3. These transitions are labeled Q(0), Q(1), Q(2), and Q(3), respectively. We also observe a transition to the F state, but do not use it.

Because the laser might have different excitation efficiencies for the various j_i, we also do a calibration with 300K H_2 gas.

APPARATUS

We use a laser with high spectral brightness that provides efficient excitation of the four H_2 transitions. This is the tunable, oscillator-amplifier combination, excimer laser (Lambda-Physik EMG-150-EST) that has four relevant features: a) a pulse energy in the range 100-200mJ, b) a bandwidth of ≈1.0cm^{-1}, c) tunability through ≈180cm^{-1}, and d) a pulse width of ≈10ns.

We made two improvements to the laser. These increased the locking of the amplifier to the oscillator and eliminated the effect of atmospheric absorption.

It is essential to have good "locking" of the amplifier to the oscillator. The part of the beam that is not locked, i.e., that is broad-band, ionizes all four H_2 transitions and this constitutes background noise. We installed a

cylindrical telescope that injected more oscillator light into the amplifier and so reduced the noise.

There are wavelength regions of such strong O_2 absorptions within our tuning range that most of the laser energy is lost in the ≈2m beam path. At the same wavelengths, there is also O_2 absorption within the oscillator and on the path to the amplifier: that yields a weaker input to the amplifier and consequently less locking. These effects distort the observed the Q(1) H_2-line. The cure was to displace the air along these paths with N_2.

The locked part of the laser beam is linearly polarized while the unlocked part is random. We sometimes insert a Rochon polarizing prism that transmits the locked portion and reduces the unlocked portion by 50%.

Figure 1 shows an apparatus schematic. The laser is triggered by an XT-clone computer. The laser beam is split: 4% goes to a Joulemeter and the remainder into an H_2 cell. Two different cells have been used. The first is a WSU-made flowing-gas cell (subsequently called WSU cell) that contains two parallel electrodes (US pennies) that are about 8mm apart. The second is a sealed Hamamatsu hollow-cathode cell (subsequently called HC cell) that contains a few torr of H_2. This is a "see-through" model whose electrodes are two coaxial hollow cylinders: the laser beam travels parallel to the same axis and does not strike the electrodes. Either cell can be operated with or without a discharge. The WSU-cell allows changes to be made in the electrode geometry and in the pressure. However the HC-cell provides a more stable discharge, is more compact, and is more convenient to use because there is no associated vacuum system.

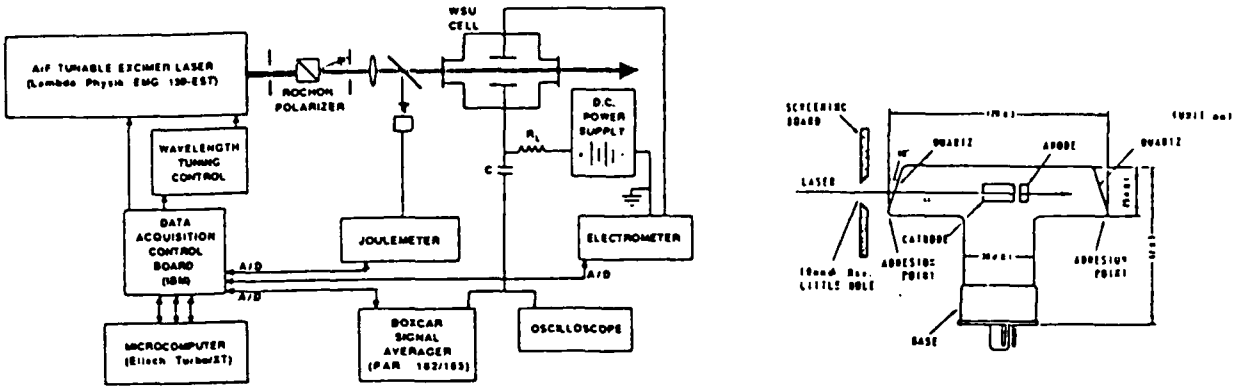

Figure 1. Left: Overall apparatus schematic including the WSU cell. Right: the Hamamatsu HC-cell.

In either cell, the laser creates H_2^*, H_2^+, and e^-. In neutral H_2, the charged particles are collected with the use of 50-150V between the electrodes. The H_2^+ current (typically 10^{-8}A) is measured with an electrometer that integrates the pulses into a dc current. Alternatively the current pulses pass through capacitor C to a boxcar signal averager that measures the voltage at a preselected time after the laser pulse. A milliammeter replaces the electrometer when the discharge is on and reads the current. Signals from the electrometer, joulemeter and boxcar, are sent to the computer.

Without a discharge, either the boxcar or the electrometer can be used, because the laser is the only source of current and there is no noise between laser shots.

The wavelength is varied by tilting a diffraction grating, that is one end of the oscillator cavity, with a micrometer screw. We attached this screw to a stepper motor that is driven by the computer. Each computer control pulse changes the wavelength by 1.87×10^{-4}nm.

A spectrum acquisition consists of the following steps. The computer is programmed to fire the laser a preselected number of times at a given wavelength. The signals from the joulemeter and boxcar (or electrometer) are stored in the

computer. The computer then turns the micrometer and the procedure is repeated at the next wavelength. This generates spectra such as those shown in Figs. 2 and 3. Depending on our purpose we can a) scan the entire spectrum at a uniform speed, b) quickly approach each of the four peaks and then scan them slowly, as in Figs. 2 and 3 or c) sit on a given peak and vary some other experimental parameters (e.g., cell pressure or laser pulse energy). Because the ion signals are roughly proportional to the square of the laser-pulse energy E, we divide each raw electrometer or boxcar output by the square of the Joulemeter output. This tends to correct for shot-to-shot laser-energy fluctuations.

Figure 2 has data from the WSU cell, with no discharge and recorded with the electrometer. Figure 3 contains data from the HC cell, both with and without a discharge using boxcar detection. It shows that much larger, but noisier, signals occur in the discharge.

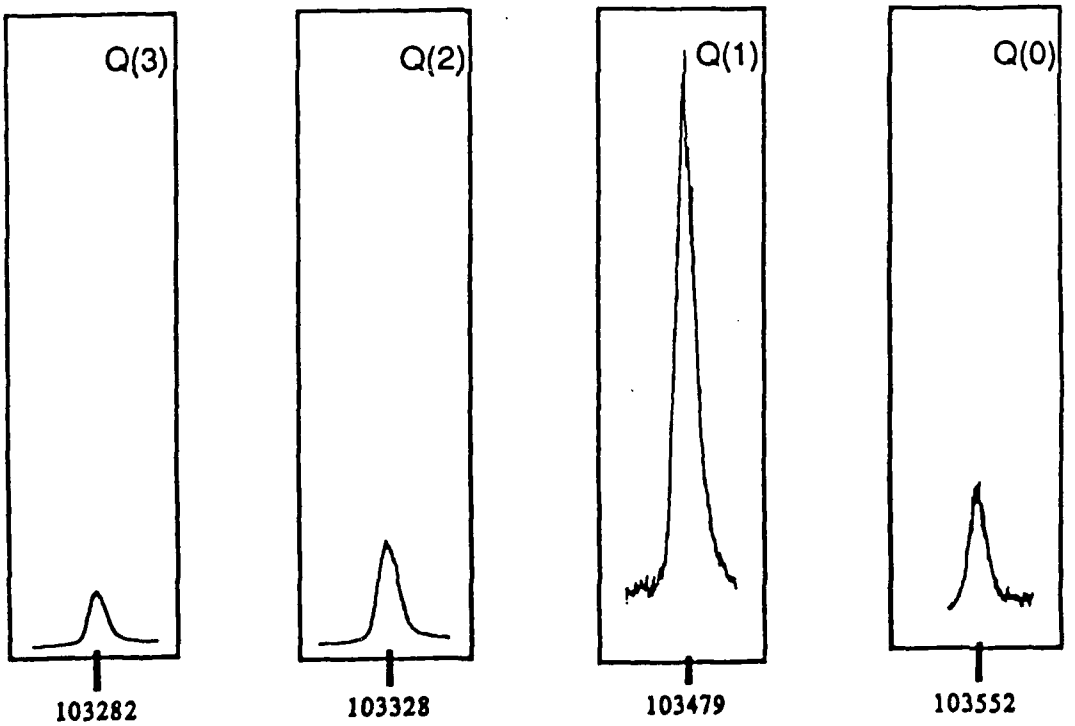

Figure 2. Peaks from the excitation of H_2 to v=2 of the E-state. The abscissa shows the energy, in cm^{-1}, of two laser photons. These data were from neutral 300K H_2, in the WSU cell, and recorded with the electrometer.

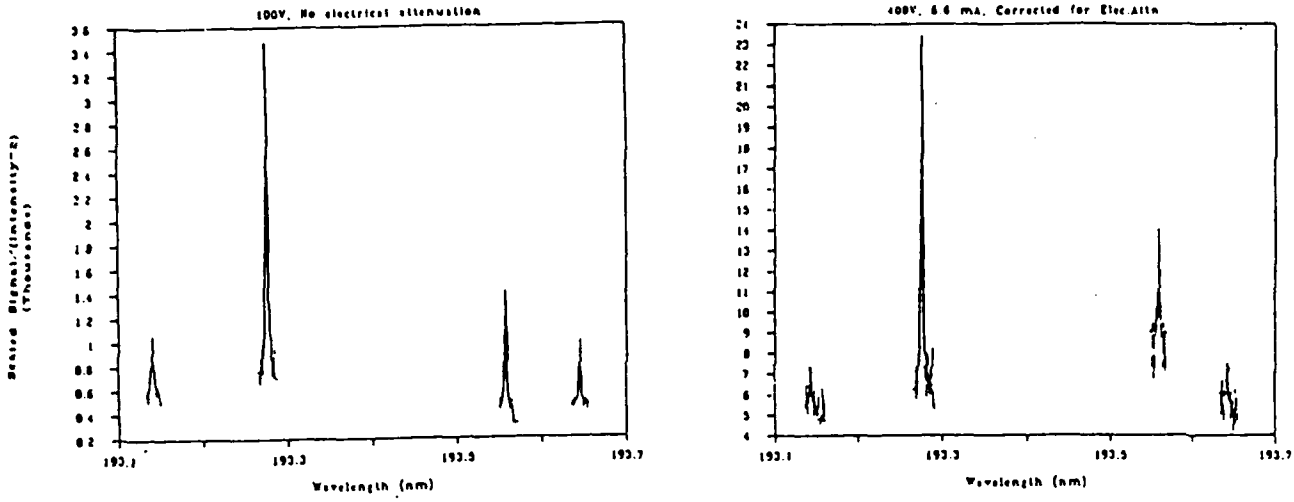

Figure 3. Peaks from the excitation of H_2 to v=2 of the E-state. The abscissa shows wavelength in nm. These data were from the HC cell, and recorded with the boxcar. At the left are results with neutral hydrogen, and at the right from a discharge. Note the bigger signals at the right.

EXPERIMENTAL PARAMETERS

We obtained results for various experimental parameters in the WSU cell with neutral gas: i.e., a) the dependence of signal upon laser energy, b) a check of the possibility of saturation, c) the effect of electrode collection voltage upon the signal and d) the effect of hydrogen pressure upon the signal.

The effect of the laser-pulse energy E upon the Q(1) signal intensity I, and upon the background B, was studied. We expected that the two-photon excitation would be the rate limiting step, so that I and B would be proportional to E^2. We found that they were $E^{1.8}$ and $E^{1.7}$, respectively.

We also checked for a saturation effect and so we used a more powerful beam. We normally limit the laser's energy by the use of an ≈1mm diam. iris before the focussing lens. By the use of a somewhat larger aperture, more energy arrives at the focus. We did find some evidence for saturation at energies higher than those normally used here.

The effect of collecting voltage upon the measured intensities was measured for all four lines. All show linear behavior below 200V, and so collection within this range will give reliable results.

The signal I initially rises with P as expected, but then reaches a maximum. It is possible that competing channels may become more effective at higher P.

NEUTRAL GAS TEMPERATURE MEASUREMENT

As an example we analyze the results of Figure 2. The cell is at room temperature, has 0.68Torr of H_2, with 50V applied to the electrodes. The ion signals are corrected by dividing by the square of the laser energy, as described above. We then find that the normalized rotational intensity distributions Q(0):Q(1):Q(2):Q(3) for the E-X (2,0) are 1:4.34:0.8:0.42. The Boltzmann prediction for 298K is 1:4.83:0.77:0.5.

We plotted $\ln[S_i/(2j_i+1)(2T_i+1)]$ versus $Bj_i(j_i+1)$, where B is the rotational constant. Linear regression was used to determine a slope that yielded T=289±20K. If we include the rotational line strengths of the molecule, the result would be 298±20K.

DISCHARGE TEMPERATURE

The laser-induced optogalvanic effect is a change in the impedance of a discharge that is induced by laser radiation of a wavelength corresponding to an atomic or molecular transition of some component of the plasma. This effect has developed into a useful spectroscopic tool in many applications.

When the cell is operated at a sufficiently high voltage, a glow discharge forms. We typically use discharge currents in the range 4-10mA. The overall potential change across the discharge that is caused by the laser is as much as 20V. In this application, the boxcar is necessary because there is a large dc noise component. Sample

measurements, on the same lines used in the neutral gas, yield a temperature of 290±50K in the discharge.

2. VIBRATIONAL ANALYSES

Volume sources for H^- have become increasingly popular. Their final mechanism to produce H^- is believed to be

$$e^- + H_2(v) \rightarrow H + H^-,$$

where $H_2(v)$ indicates various vibrational states of hydrogen. The cross section for this process appears to be three to four orders of magnitude higher for v=5 than for v=0. In order to design such sources, it is desirable to have an appropriate monitor for $H_2(v)$.

The same (2+1) REMPI method that was used for the discharge is being used here. The difference is that the transition frequencies needed for the $H_2(v)$ are shifted. For example, for monitoring $H_2(2)$ two vibrational quanta less energy are needed to reach the same upper state as with the 193nm. This frequency shift is done by focussing the excimer light into a "Raman cell" that contains 20-40bar of H_2. The light leaving the Raman cell contains the original frequency as well those that have 1, 2, 3, etc. vibrational quanta smaller frequency, called the 1st, 2nd, 3rd, etc. Stokes frequencies, respectively. These components are separated with a Pellin-Broca prism.

For example a 2+1 REMPI on $H_2(0)$, going to v=2 of the E state is accomplished with 193nm light, as described above. Similarly, starting with H_2 (v=2), approximately the same energy would be reached by two photons of the first Stokes frequency. (It would be exactly the same if the H_2 potential well were a harmonic oscillator), and calculations with H_2 and with D_2 in the Raman cell show that there are many appropriate lines for analysis of $H_2(v)$. Figure 4 shows some of these line positions for the first Stokes in an H_2 cell. We have constructed a Raman cell and have ≈5mJ of first Stokes light.

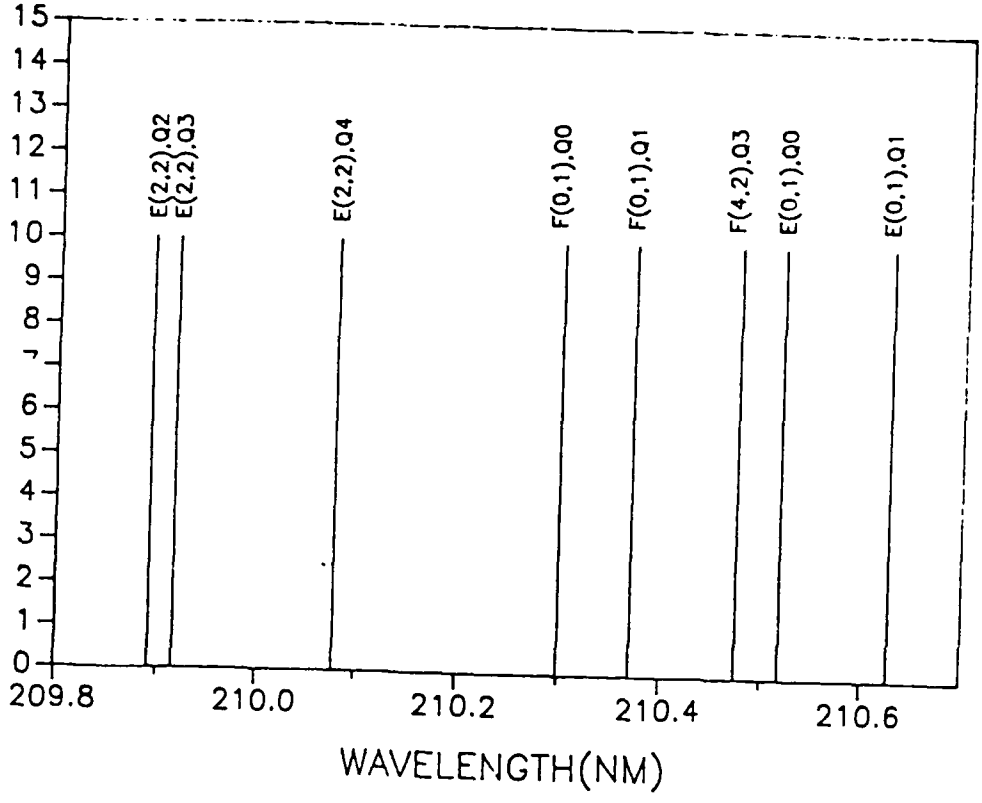

Figure 4. Line positions, but not heights, for 2+1 REMPI (to E or F states) of H_2 using Raman-shifted 1st-Stokes excitation. This assumes a Raman cell filled with H_2, using the 193nm band excitation.

INTRODUCTION TO FORMATION OF VIBRATIONALLY EXCITED H_2

Meier, et al.[3] prepared X-state H_2 in the single rotational level v"=1, J"=1 [hereafter called $H_2(1,1)$] by stimulated Raman pumping with IR light. They injected fundamental Nd-YAG laser light at $\tilde{\nu}_r$=9396.55cm^{-1} into an H_2-filled Raman shifter. Some of the beam that emerged was the first Stokes at $\tilde{\nu}_{s1}$=5241.30cm^{-1}. The energy difference, $\tilde{\nu}_r$-$\tilde{\nu}_{s1}$=4155.25cm^{-1}, is that between the v"=0, J"=1 and $H_2(1,1)$ states.[4] They made $H_2(1,1)$ by focussing light of $\tilde{\nu}_r$ and $\tilde{\nu}_{s1}$ into an H_2-filled region. The state distribution was measured with LIF that used tunable VUV (λ≈110nm) light.

Here we describe the use a single tunable ArF laser and a Raman shifter to simultaneously a) populate $H_2(1,1)$ via stimulated Raman pumping with UV-light, and b) to detect

that $H_2(1,1)$ by means of (2+1) REMPI via the EF-state. When the laser wavelength is tuned through its range, the amount of $H_2(1,1)$ formed varies only slowly, but a structured REMPI spectrum is seen.

The two-photon spectral lines are easily identified because the X-state[5] and the EF-state[6,7] energy levels are precisely known, and because such (2+1) REMPI has been previously reported.[1,7-11]

EXPERIMENTAL APPROACH

Figure 5 is a schematic of the apparatus. Narrow-band ArF light, at a selected $\tilde{\nu}_F$, is focussed (f=89cm) into a 90cm long Raman shifter that has fused silica windows. When it contains H_2, a mixture of light emerges that includes $\tilde{\nu}_F$ and $\tilde{\nu}_{S1}$. The $\tilde{\nu}_{S1}$ are in the $\lambda_{S1}\approx 210$nm range. The difference $\tilde{\nu}_F - \tilde{\nu}_{S1} = 4155.25\text{cm}^{-1}$ is independent of ν_F. The longer Stokes wavelengths λ_{S2} and λ_{S3} are also present but any anti-Stokes light is absorbed by the windows.

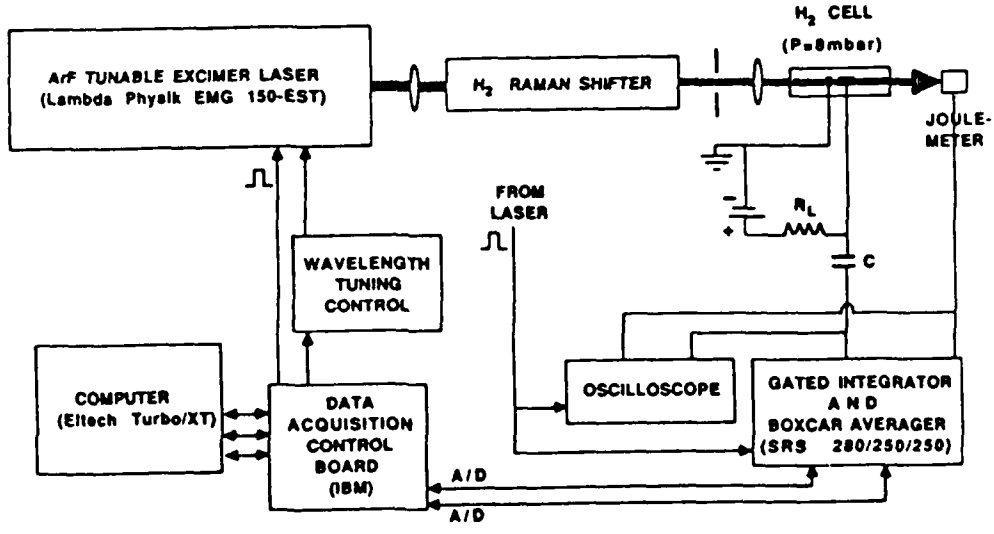

Fig. 5. Schematic of the apparatus. The drawing is not to scale.

The emerging light is focussed into ≈8mbar of H_2 at 300K. The focal length of the fused silica lens is λ-dependent: $f(\lambda_{si})\approx 23cm$ and $f(\lambda_F)\approx 22cm$. The H_2 is sealed inside a Hamamatsu "see-through" cell that has fused silica entrance and exit windows. The light goes through it along the axis of two hollow cylindrical electrodes without striking them. REMPI electron pulses are collected with ≈100V. They are transmitted by a capacitor to an oscilloscope and a boxcar signal averager that have one megohm input impedances. The laser energy after the cell is measured with a joulemeter.

The laser is an oscillator-amplifier combination that has a) a pulse energy I_F in the range 100-300mJ, b) a bandwidth of ≈0.003nm, c) tunability between $\lambda_F \approx 193.1$-193.8nm, d) linear polarization of the narrow band portion, and e) a pulse width of ≈15ns. It is typically used at a repetition rate of 1-2Hz. An adjustable iris limits the energy and size of the laser beam.

We adjust λ_F by tilting a grating in the oscillator cavity with a micrometer screw. That screw connected to a stepper motor by a home-made linkage. Hysteresis in the linkage limits the measurement of relative λ_F to ≈0.002nm.

An XT-clone computer controls spectrum acquisition. It fires the laser a preselected number of times (usually 7) at a given λ_F. The signals from the joulemeter and boxcar are stored in the computer. The computer then changes λ_F by a nominal 1.87×10^{-4}nm and the procedure is repeated. We either a) scan the λ_F-region at a uniform speed and generate spectra such as those in Figs. 6 and 7 or b) quickly approach each REMPI peak and then scan it slowly. Method a) is longer, but it is better for determinations of λ_F because there is less linkage hysteresis. Method b) is best for measuring relative REMPI peak heights because the laser's energy, and its degree of locking, decrease with time as its gases age.

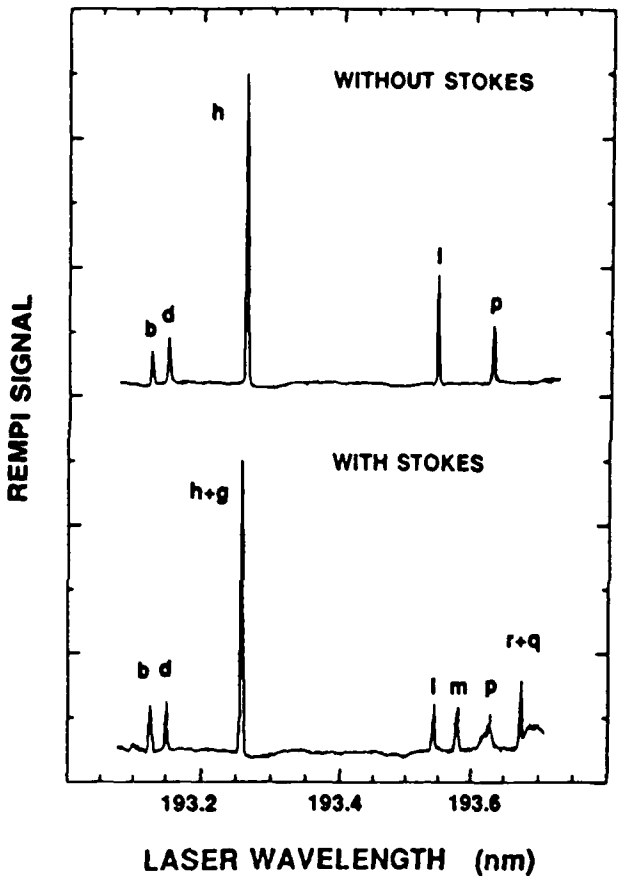

Figure 6

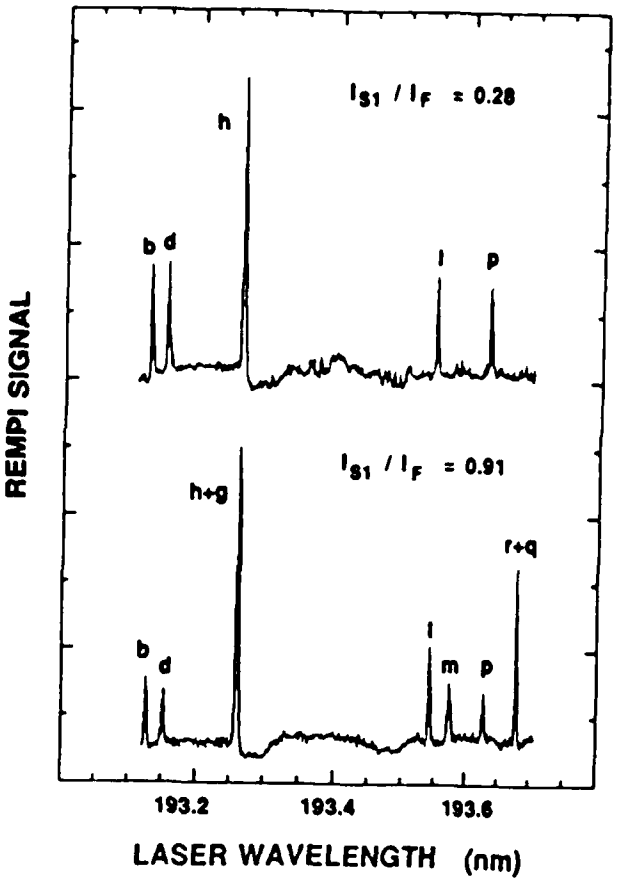

Figure 7

Fig. 6. (2+1) REMPI spectra from H_2 using narrow-band laser light. Top: Only 193nm-range light is used. The five lines are all from v"=0. Bottom: 210nm-range Stokes light is added to the 193nm fundamental. The letters refer to transitions listed in Table I. Each spectrum has been normalized and peak heights between the two should not be compared. The unevenness in the baseline is from broad-line atmospheric O_2 absorption.

Fig. 7 (2+1) REMPI spectra from two different mixtures of tuned 193nm- and 210nm-range laser.

We compare REMPI spectra at different values of I_F/I_{S1}. This intensity ratio is adjusted by varying the Raman shifter's H_2 pressure and it is measured by inserting a Pellin-Broca prism (not shown in Fig. 1) to physically separate the beams of λ_F and λ_{S1}. Because $I_{S1}=0$ when Ar is substituted for the shifter's H_2, only transitions from v"=0, via $\tilde{\nu}_F+\tilde{\nu}_F$, will occur. With H_2 in the shifter, there are extra lines from v"=0, via $\tilde{\nu}_{S1}+\tilde{\nu}_{S1}$ and $\tilde{\nu}_F+\tilde{\nu}_{S1}$, and from $H_2(1,1)$.

RESULTS AND DISCUSSION

Figure 6 shows REMPI spectra obtained a) with Ar and b) with H_2 in the Raman shifter. Figure 7 has similar spectra at two different ratios I_F/I_{S1}. These spectra were acquired with method a) above. They are not corrected for I_F variations. There are two additional lines when H_2 is in the shifter.

Table I lists all EF-X, two-photon, Q-transitions that might occur within our λ_F range. The λ_F and λ_{S1} are derived from term energies listed in Dabrowski's[5] Table 5 and in Senn and Dressler's[6] Table V. The most relevant transitions are pictured in Fig. 8.

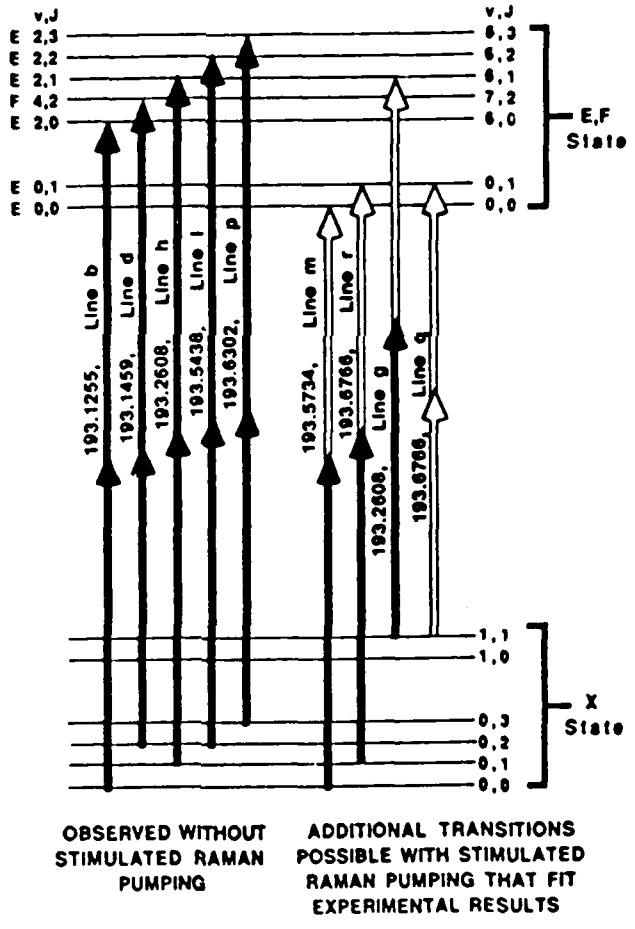

Fig. 8 Term diagram showing relevant two-photon EF<--X transitions. At the left are those occurring without Stokes light. Solid and open arrows indicate 193nm and 210nm range photons, respectively.

Table I

All possible two-photon Q-transitions (J≡J"=J') within our λ_F-range. Wavelengths are calculated from refs. 3 and 4. The v' are in the EF-state notation used in ref. 4, while "Upper state" numbers are for the individual E and F wells. WR and WOR mean observed with and without Raman shifting, respectively, and NO means not observed. In comments that justify NO, a) transitions to F0 are improbable (see text) and b) production of v"=1 occurs only for J=1.

	Photon pair	v"	v'	J	λ_F	λ_S	Upper state	Comments
a	F+S	1	7	2	193.1240	209.9739	F4	NO, overlaps b, v"=1,J=2
b	2F	0	6	0	193.1255	--------	E2	WOR
c	F+S	1	6	0	193.1365	209.9888	E2	NO, v"=1,J=0
d	2F	0	7	2	193.1459	--------	F4	WOR
e	F+S	0	1	0	193.2009	210.0649	F0	NO, F0
f	2S	1	1	0	193.2119	210.0779	F0	NO, F0
g	F+S	1	6	1	193.2608	210.1357	E2	overlaps h
h	2F	0	6	1	193.2608	--------	E2	WOR, overlaps g
i	F+S	0	1	1	193.3997	210.2999	F0	NO, F0
j	2S	1	1	1	193.3997	210.2999	F0	NO, F0
k	F+S	1	6	2	193.5218	210.4442	E2	v"=1,J=2
l	2F	0	6	2	193.5438	--------	E2	WOR
m	F+S	0	0	0	193.5734	210.5053	E0	WR
n	F+S	1	7	3	193.5752	210.5074	E2	NO, v"=1,J=3
o	2S	1	0	0	193.5844	210.5183	E0	NO, v"=1,J=0
p	2F	0	7	3	193.6302	--------	E2	WOR
q	2S	1	0	1	193.6766	210.6273	E0	WR, overlaps r
r	F+S	0	0	1	193.6766	210.6273	E0	WR, overlaps q
s	2S	1	1	2	193.7737	210.7422	F0	NO, v"=1,J=2

Marinero, et al.[1] have discussed the EF-state and showed that Q-transitions dominate the (2+1) REMPI spectrum via that state. The EF-state has a double minimum. The well of the inner E-state contains three vibrational levels and that of the outer F-state has five.[3,8] For example, transition a in Table I is to F4: i.e., That is the upper level of the F-state. Alternative labels[6] are in use that recognize EF as a single state whose vibrational levels are numbered in order of increasing energy. Both notations are used in Table I and in Fig. 8.

Without $\tilde{\nu}_{S1}$, the REMPI spectrum consists of the five often observed[1,2,7-10] transitions (b, d, h, l, and p) induced by $\tilde{\nu}_F+\tilde{\nu}_F$. These are pictured at the top of Fig. 6 and the left side of Fig. 8. They are Q(0), Q(1), Q(2), and Q(3) to E2 and Q(2) to F4. These lines serve to calibrate the wavelength scale of the laser.

Marinero, et al.[1] found no transitions to the F0 state because, they said, there is only a small vibrational overlap. Our data are consistent with theirs. Transitions e, f, i, j, and s of Table I are to F0 and we do not see them.

When both $\tilde{\nu}_F$ and $\tilde{\nu}_{S1}$ are present, we a) produce $H_2(1,1)$ and can do REMPI from that and/or b) we add the possibility of $\tilde{\nu}_F+\tilde{\nu}_{S1}$ and $\tilde{\nu}_{S1}+\tilde{\nu}_{S1}$ transitions.

Meier, et al.[3] reported that only $H_2(1,1)$ is made by the stimulated Raman pumping and we find the same result. For example, the calculated transition k is from v"=1, J"=J=2 to the same upper state E2 as transition l. However it is not observed and this indicates that v"=1, J=2 is not made. Similarly, the lack of transitions c and o means that there is no v"=1, J=0. This reasoning is less persuasive with transitions a or s, because line a nearly overlaps line b, and because line s goes to F0, which would be unlikely (see above) even if v"=1, J=2 were formed.

In Fig. 7, with Raman shifting, we see two new lines. Because of energy-degeneracy in the shifting-REMPI

combinations, some discussion is required. Figure 8 shows the problem. One of the new peaks is at λ_r=193.6766nm, which must be transitions q and/or r. These begin at v"=1, J=1 and at E0, J=1, respectively, and both end at v'=0, J'=1. Transition q needs energy $\tilde{\nu}_{s1}+\tilde{\nu}_{s1}$, while r requires $\tilde{\nu}_{s1}+\tilde{\nu}_r$. The energy difference a) between the fundamental and first Stokes photons is $\tilde{\nu}_{s1}-\tilde{\nu}_r$, and b) between the transition energies for q and r is also $\tilde{\nu}_{s1}-\tilde{\nu}_r$. That means that λ_r for q and r is the same. Similarly, transitions g and h are from the same lower states as q and r, but go to E2 and both have λ_r=193.2608nm. Because h involves $\tilde{\nu}_r+\tilde{\nu}_r$ this is *not* a new line: it occurs without Raman shifting. The only other possible transition from $H_2(1,1)$, i.e., j, would go to F0 but those lines (see above) are never observed.

The second new line, m, at λ=193.5734 has no ambiguity: it is caused by $\tilde{\nu}_r+\tilde{\nu}_{s1}$. However because it begins at v"=0, J=0, it is unrelated to the presence of $H_2(1,1)$.

It might be thought that the relative contributions of, e.g., q and r, could be sorted out by variation of $I_{s1}\backslash I_r$. There are however three complications: 1) the transition strengths from $H_2(1,1)$ are unknown, 2) the fraction of the I that are locked (and thus cause the REMPI spectra) are not known , and c) the shot-to-shot variations in I_r cause large REMPI fluctuations because all the processes are multiphoton.

However relative peak heights H can yield a rough estimate of the $H_2(1,1)$ population. We use three simplifying assumptions. 1) The H are a measure of line intensity. 2) The I_r and I_{s1} remain constant within the tuning range. 3) The REMPI signal has the same functional dependence upon I (e.g., I^3) for all lines excited by either $\tilde{\nu}_r+\tilde{\nu}_r$, $\tilde{\nu}_r+\tilde{\nu}_{s1}$, or $\tilde{\nu}_{s1}+\tilde{\nu}_{s1}$, these are labeled $f(I_r)$, $f(I_{r+s1})$ and $f(I_{s1})$.

At any λ, the peak height $=H_J$ is a sum of terms $f(I)\cdot{}^{=}s_J\cdot n_J$, where z represents a transition letter from

Table I and ${}^{r}s_J$ and n_J are the line strengths and the populations before pumping. A * or ** means that it refers to $H_2(1,1)$. Three relevant ratios, ${}^{m}s_o n_o/{}^{1}s_2 n_2=6.2/7.7$, ${}^{h}s_1 n_1/{}^{1}s_2 n_2=34.5/7.7$, and ${}^{r}s_1 n_1/{}^{1}s_2 n_2=27.3/7.7$ are available from Table 3 of Marinero, et al.[1] Expressions for ${}^{r}H_J$ for some single and overlapping transitions follow:

${}^{h+q}H_1 = f(I_F)\,{}^{h}s_1(n_1-n_1^*)+f(I_{F+S1})\,{}^{q}s_1^*n_1^*$ [h+g, 193.2608nm]

${}^{1}H_2 = f(I_F)\,{}^{1}s_2 n_2$ [1, 193.5438nm]

${}^{m}H_o = f(I_{F+S1})\,{}^{m}s_o n_o$ [m, 193.5734nm]

${}^{r+q}H_1 = f(I_{F+S1})\,{}^{r}s_1(n_1-n_1^*)+f(I_{S1})\,{}^{q}s_1^{**}n_1^*$ [r+q, 193.6766nm]

In order to estimate n_1^*, we need $\Phi\equiv f(I_{F+S1})/f(I_F)$ at some particular set of laser parameters. Transitions m and 1 occur from J=0 and 2, which are not Raman pumped. The measured ratio ${}^{m}H_o/{}^{1}H_2$ is $\Phi[{}^{m}s_o n_o/{}^{1}s_2 n_2]=6.2\Phi/7.7$, and so Φ is available from the data.

Because J=1 is Raman pumped and J=2 is not, we can estimate n_1^*. We define R to be ${}^{q+h}H_1/{}^{1}H_2={}^{h}s_1 n_1/{}^{1}s_2 n_2+({}^{q}s_1^*\Phi-{}^{h}s_1)n_1^*/{}^{1}s_2 n_2$. Let R^o be R when $n_1^*=0$, *i.e., with Ar in the shifter.* Then $R-R^o=({}^{q}s_1^*\Phi-{}^{h}s_1)n_1^*/{}^{1}s_2 n_2=[({}^{q}s_1^*\Phi/{}^{h}s_1)-1](n_1^*/n_1)({}^{h}s_1 n_1/{}^{1}s_2 n_2)$, so that $n_1^*/n_1=7.7(R-R^o)/\{34.5[({}^{q}s_1^*\Phi/{}^{h}s_1)-1]\}$. We now assume that ${}^{q}s_1^*={}^{h}s_1$, because we have no better information.

We measure the relative H using method b) described above, i.e., a slow scan of the peaks only. From the above equations, for $I_{S1}/I_F=0.91$ and 0.28, the respective Φ are 0.6 and 0.06, the $R-R^o$ are -1.13 and -1.61, and the n_1^*/n_1 are 0.63 and 0.38. These are crude values, but they do show that large fractions of v"=0, J=1 are excited to $H_2(1,1)$, and that, as expected, the fraction is larger at greater I_{S1}/I_F.

Finally we consider the r+q peak, which is absent without v_{S1}, and so it is more difficult to analyze. Let $R'\equiv {}^{r+q}H_1/{}^{1}H_2=\Phi({}^{r}s_1 n_1/{}^{1}s_2 n_2)+\{[f(I_{S1})/f(I_F)]\,{}^{q}s_1^{**}-\Phi\,{}^{r}s_1\}n_1^*/{}^{1}s_2 n_2$, so that $R'/\Phi=(27.3/7.7)+[(\Phi'\,{}^{q}s_1^{**}-{}^{r}s_1)n_1^*/{}^{1}s_2 n_2]$, where $\Phi'\equiv f(I_{S1})/f(I_{F+S1})$. Because we can not measure Φ', we have not obtained a value for n_1^*.

However when $n_1^*=0$, R'/Φ is independent of these factors. From the data, when I_{S1}/I_F = 0.28 and 0.91 and the calculated Φ were 0.06 and 0.6, the corresponding R'/Φ were 1.7 and 3.1, respectively. This change comes because a) n_1^* increases, and b) Φ' must go up at larger I_{S1}/I_F. The expression for R'/Φ can be simplified to $(27.3/7.7)[1+(\Phi'-1)(n_1^*/n_1)]$ by assuming that $\sigma_{S_1^*}=\sigma_{S_1}$, but Φ' is still unknown.

SUMMARY OF PRODUCTION AND MEASUREMENT OF VIBRATIONAL EXCITATION

We use a tunable ArF laser combined with a Raman shifter to produce $H_2(1,1)$ via stimulated Raman pumping. A qualitative analysis is simultaneously performed using the same laser via REMPI spectra. The addition of Stokes light to the fundamental laser frequency produces two new lines. One of these is two-color REMPI from v"=0, J=0, the other includes REMPI from $H_2(1,1)$. A comparison of relative peak heights, of the spectrum with only ν_F with that when Stokes light is added, shows that a significant fraction of v"=0, J=1 is prepared. As expected, there is no evidence for stimulated pumping to other rotational states of v"=1.

The experimental arrangement is simpler than that described in Ref. 3 and leads to good $H_2(1,1)$ populations. However it is less accurate. It has less versatility than the use of separate lasers because a) the frequency degeneracy leads to a more complicated state analysis that yields only qualitative results and b) no adjustable time delay is available for a probe.

Finally the results show that the REMPI is sensitive to $H_2(1,1)$, and we would expect this to be a good method for analysis of vibrational and rotational state distributions of H_2 that originate from other processes. Whether the fundamental and Stokes beams should be kept together as was done here, or separated, would depend on the particular state. The different foci for the different colors mean

that separate beams of v_r and v_{s1} would yield an extra degree of freedom. Calculations of the appropriate line strengths from excited vibrational levels would be helpful.

3. SUMMARY AND RECOMMENDATIONS FOR FUTURE WORK

The REMPI method used here has been shown to work on measurements of temperature and for analysis of vibrationally excited H_2. These diagnoses were done as local point measurements: i.e., they occur at spots where the laser light reaches a focus.

I believe it is now time to move into imaging of the sources: i.e., to develop a method whereby a distribution of molecular densities can be captured as an image.

The main advantage of the use of imaging is that simultaneous information is obtained for an entire region and not just for one point. Examples include normal camera snapshots, a variety of medical diagnostics images (like X-rays, magnetic resonance, and CAT scans), and maps of temperature distributions *from* satellite IR photographs.

This would be done with the same two-photon excitations described above, but the fluorescence would be measured. The tuned laser beam excites molecules from a state i into a higher state i^*. The number of i^* formed by the laser are proportional to n_i, the density in state i.

Those i^* that emit light do so at a limited number of frequencies. There is a two-stage selection of species to be analyzed: i.e., a) tuning of the laser in excitation and b) choice of an appropriate emission frequency. If two species were excited at the same laser wavelength, then an appropriate camera filter would be selected that passes light only from the desired specie. This allows a particular quantum state to be unambiguously analyzed within a complicated mixture.

The basic 2-D imaging technique for scattered light involves a ribbon of pulsed laser-light passing through a medium. Fluorescence light is recorded by an intensified

CCD camera pointed at 90° to the path of the light-ribbon. One laser function is to be a "flashbulb" that determines the time scale. Our laser pulse lasts ≈15ns. This is essentially "stop action" even with a worst case that has molecular velocities. For example, at one km/s, the molecule moves only ≈15μm during the pulse. [Future 3-D imaging will involve rapid scanning through different planes.]

Recently CCD-based imagers became popular because of the consumer market for TV cameras. By combining CCD-cameras with image-intensifiers that were originally developed for "night vision" purposes, extremely low light levels could be measured. As a result, research that might have formerly involved collection of light from a point, and of measurement of its intensity with a photomultiplier, can now be done simultaneously at a large number of points as a 2-D image. For measurements that are based on scattered light, imaging will yield significantly more information.

Finally, images obtained from the CCD cameras can be acquired and processed with AT-type personal computers that are equipped with one or two of a large selection of picture-acquisition and processing PC-boards that can be purchased at a modest cost.

4. REFERENCES

1. E.E. Marinero, C.T. Rettner, and R.N. Zare, Phys. Rev. Lett. **48**, 1323 (1982); E.E. Marinero, R. Vasudev, and R.N. Zare, J. Chem. Phys. **78** 692 (1983).

2. E.W. Rothe, G.S. Ondrey, and P. Andresen, Optics Comm. **58**, 113 (1986).

3. W. Meier, G. Ahlers, and H. Zacharias, J. Chem. Phys. **85**, 2599 (1986).

4. S. L. Bragg, J. W. Brault, and W. H. Smith, Astrophys. J. **263**, 999 (1982).

5. I. Dabrowski, Can. J. Phys. **62**, 1639 (1984).

6. P. Senn and K. Dressler, J. Chem. Phys. **87**, 6908 (1987).

7. E. E. Eyler, J. Gilligan, E. McCormack, A. Nussenzweig, and E. Pollack, Phys. Rev. **A36**, 3486 (1987).

8. D. J. Kligler and C. K. Rhodes, Phys. Rev. Lett. **40**, 309 (1978).

9. D. J. Kligler, J. Bokor, and C. K. Rhodes, Phys. Rev. **A21**, 607 (1980).

10. L.M. Hitchcock, G.P. Reck, E.W. Rothe, and C.C. Tung, Microwave and Particle Beam Sources, SPIE **1061**, 621 (1989).

5. PUBLISHED PAPERS

E. W. Rothe, G. S. Ondrey and P. Andresen, "High Sensitivity, State-Specific Detection of H_2 by Three-Photon Direct Ionization in Gases and Discharges," Optics Comm. 58, 113 (1986).

E. W. Rothe, R. Theyunni, G.P. Reck and C.C. Tung, "Effect of Electronic Alignment," Phys. Rev. A33, 1426 (1986).

S. P. Lee, E. W. Rothe and G. P. Reck, "Influence of Electrical Resonance Upon Interpretation of Optogalvanic Data," J. Appl. Phys. 61, 109 (1987).

S. Deshmukh, S. P. Lee, G. P. Reck and E. W. Rothe, "Optogalvanic OH (A-X) Spectrum," J. Quant. Spectrosc. Rad. Transfer 39, 339 (1988).

T. Seelemann, P. Andresen and E. W. Rothe, "Resonance Enhanced Multiphoton Ionization of Vibrationally Excited State Selected NH_3: Spectroscopy and Collisional State Transfer," Chem. Phys. Letters 146, 89 (1988).

C. C. Tung, G. P. Reck and E. W. Rothe, "Crossed Beam Study of Na^* ($^2P_{3/2}$) + O_2 --> Na^+ + O_2^-. The Dependence of the Total Cross Section upon Alignment," J. Chem. Phys. 88, 5981 (1988).

S. P. Lee, E. W. Rothe and G. P. Reck, "Resonance Enhanced Multiphoton Ionization (2 + 1) in NH_3 using Linearly and Circularly Polarized Light," Chem. Phys. 126, 145 (1988).

P. Andresen and E. W. Rothe, "Polarized Absorption Spectroscopy of Lambda-doublet Molecules: Transition Moment vs Electron Density Distribution," J. Chem. Phys. 89, 5965 (1988).

S. Deshmukh, E. W. Rothe, G. P. Reck, T. Kushida and Z. G. Xu, "Emission Spectra from ArF Laser Ablation of High T_c Superconductor $Bi_2CaSr_2Cu_2O_9$," Appl. Phys. Lett. 53, 2698 (1988).

S. Deshmukh, E. W. Rothe, G. P. Reck, T. Kushida and Z. G. Xu, "ArF Laser Induced Emission from High T_c Superconducting Thin Films Deposited by Laser Ablation," Supercond. Sci. Technol 1, 319 (1989).

L.M. Hitchcock, G.P. Reck, E.W. Rothe, and C.C. Tung, Microwave and Particle Beam Sources, SPIE 1061, 621 (1989).

S. Deshmukh, E. W. Rothe, and G. P. Reck, "Photoablation of Polymers at 193nm: Shot-to-Shot Study of Emission Spectra, Etch Depths, and Transmission," J. Appl. Phys. 66, 1370 (1989).

P. Andresen, G. Meijer, H Schlüter, H. Voges, A. Koch, W. Hentschel, W. Oppermann, and E. W. Rothe, "Fluorescence Imaging Inside an Internal Combustion Engine using Tunable Excimer Lasers," Applied Optics (scheduled to appear 1 June 1990).

L. M. Hitchcock, G. S. Kim, G. P. Reck, and E. W. Rothe, "Absorption of Laser Light in Air in the 193nm Range: Analysis of Laser Locking," J. Quant. Spectrosc. Rad. Transfer (accepted for publication).

L. M. Hitchcock, G. S. Kim, E. W. Rothe, and G. P. Reck, "Formation of H_2 (v"=1, J"=1) and (2+1) REMPI from it using a Single Tunable ArF Excimer Laser, J. Chem. Phys. (submitted).

6. PERSONNEL

The following personnel have worked on the project

Senior Personnel
E. W. Rothe, Professor of Engineering, P.I.
G. P. Reck, Professor of Chemistry

Postdoctoral Associate
L. Hitchcock

Graduate Students who obtained a Ph.D.
S. Deshmukh
S.P. Lee
C.C. Tung

Graduate Students who obtained a Masters
A. Fawaz
A. Modi
M. Han

Graduate Student in last phase of Ph.D. work
G. Kim